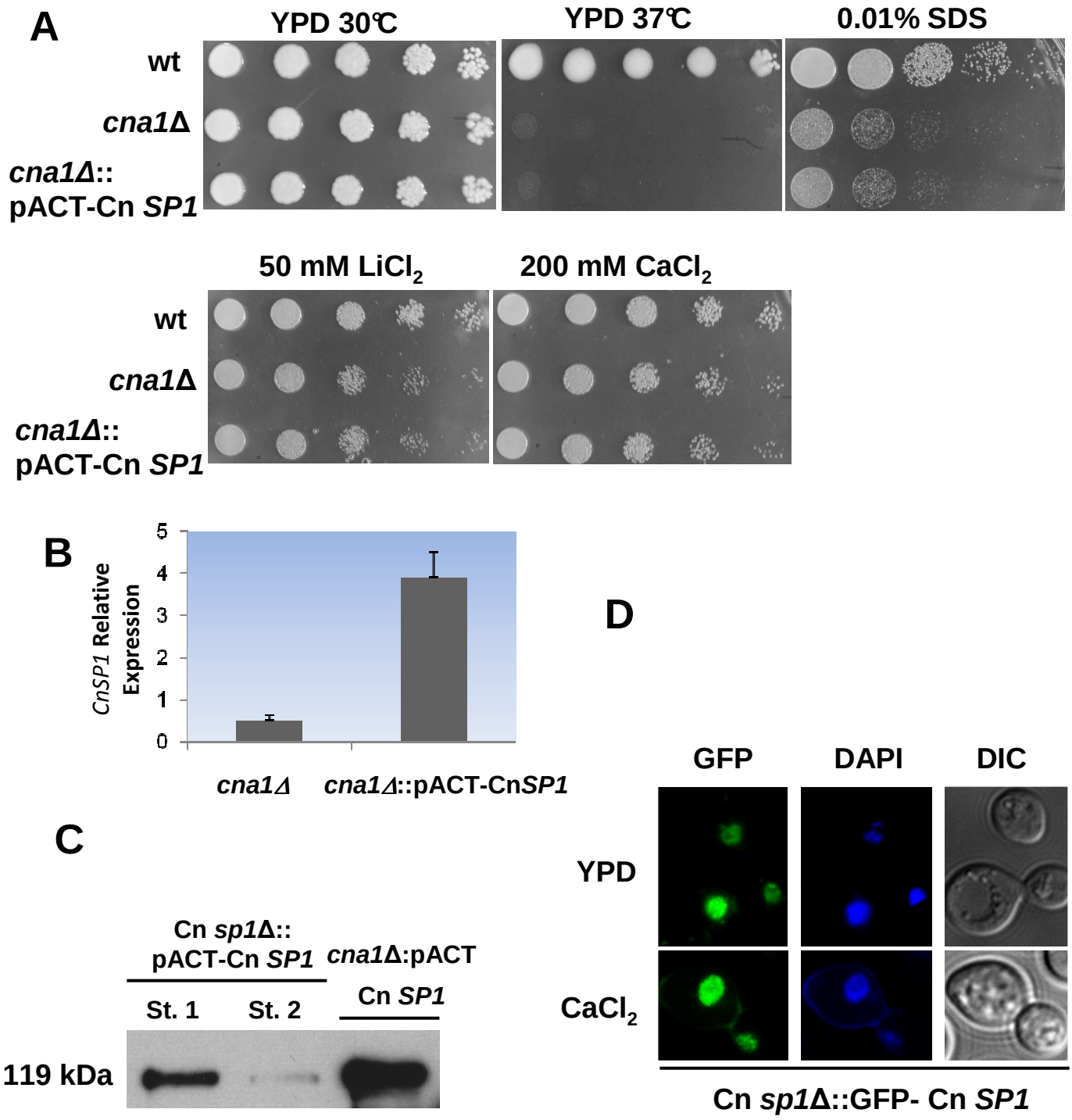

Figure S1. *CNAG_00156* (Cn *SP1*) is not the *C. neoformans CRZ1*.
(A) WT, *cna1*Δ, and *cna1*Δ:pACT-Cn *SP1* strains were grown on YPD + sorbitol media and suspended in PBS media to OD_{600} of 0.1. Five 5-fold dilutions of each strain were spotted on the various media and observed for 48 hours. **(B)** shows validation by qRT-PCR of Cn *SP1* over-expression in the *cna1*Δ:pACT-Cn *SP1* strain. Values are ratios of expression of Cn *SP1* transcript to *ACT1*.
(C) Cn *sp1Δ*:pACT-Cn *SP1* (2 strains: st. 1 and St. 2) and *cnaΔ*:pACT-Cn *SP1* strains (all containing a *c-myc* tag, see 'Experimental Procedures') were grown in YPD to an OD600 of 0.4-0.6, lysed and immunoprecipitated with anti *c-myc* antibodies. Protein eluents were resolved on a SDS-PAGE gel. **(D)** Cn *sp1Δ*:GFP-Cn *SP1* cells were grown in YPD to mid-log, and viewed with a confocal fluorescent microscope before and after addition of 20 mM $CaCl_2$. Nuclear localization of Cn Sp1 was observed independent of $CaCl_2$.

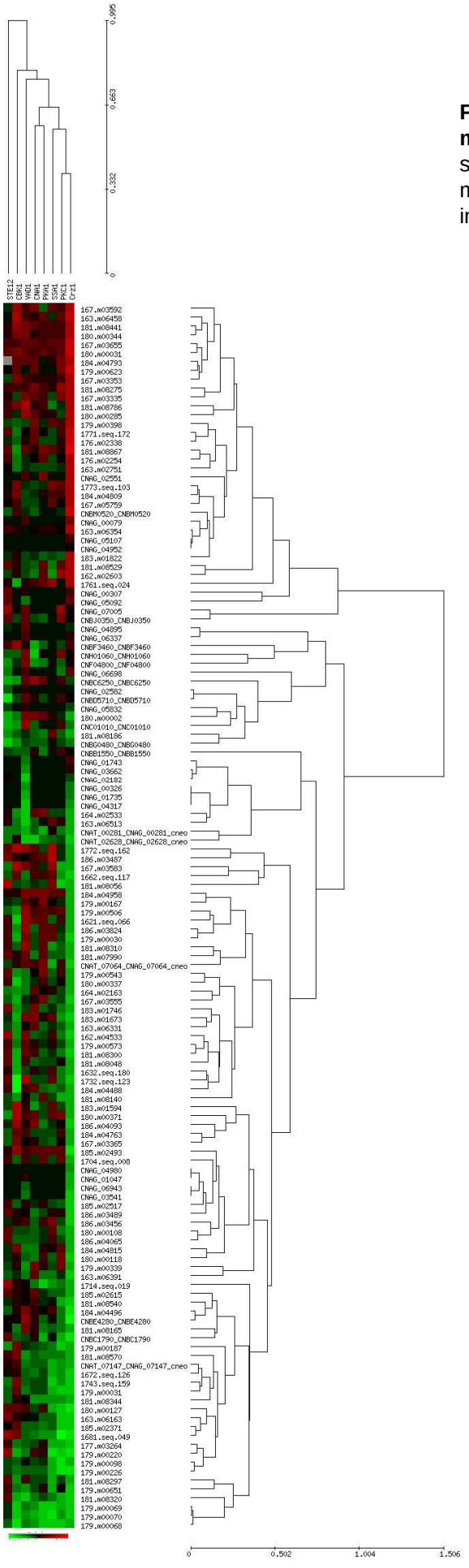

Figure S2: Transcriptional comparison of cryptococcal mutants under starvation conditions. Indicated strains were subjected to starvation and RNA prepared and subjected to microarray analysis using glass slide arrays as described in “Materials and Methods”.

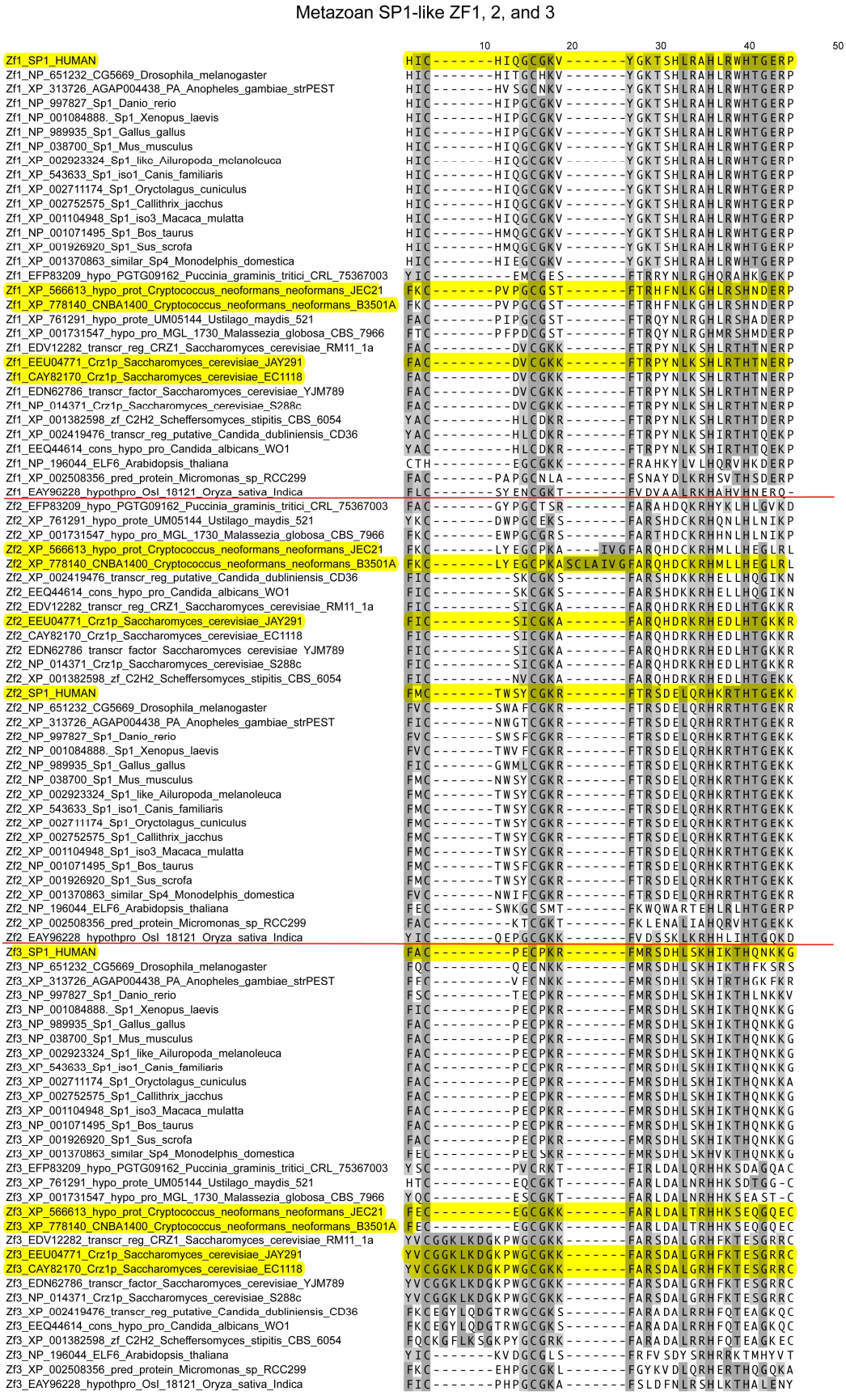

Figure S3a: Sequence alignment of Zn finger regions and associated sequences of fungi and metazoans Representative Sp1, Crz1 and Cn Sp1-like protein sequences were retrieved from a BLASTp (ref) search. Full protein sequences were aligned using the MUSCLE software (ref) and individual zinc-finger motifs were identified and extracted. A multiple sequence alignment of the three zinc-finger motifs was created manually based on the MUSCLE alignment.

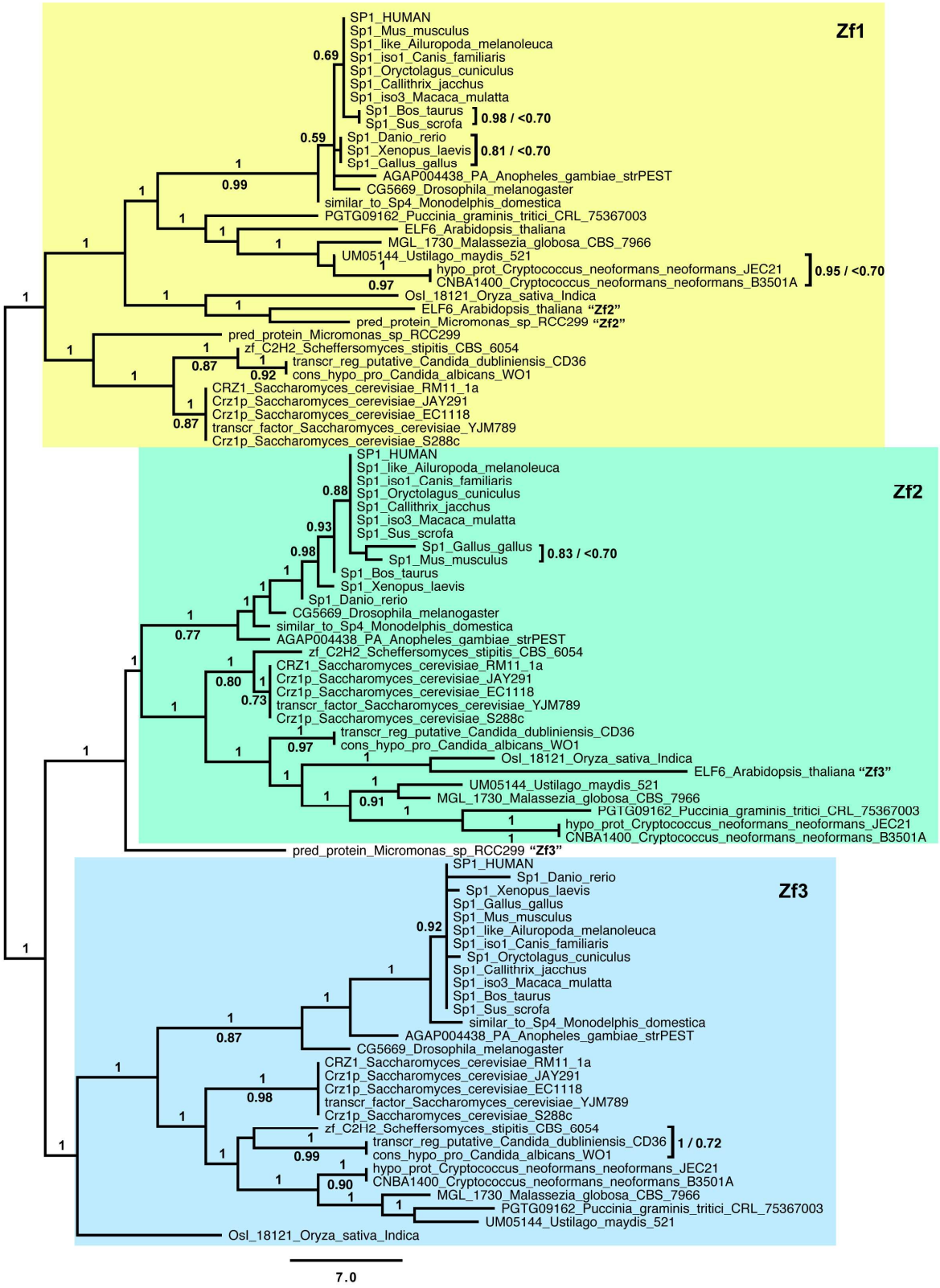

Figure S3b:Parimonious trees constructed from sequences aligned in Figure S3a. Sequences from Figure S3a were submitted to PAUP (ref) and a heuristic search for the most parsimonious tree was performed. PAUP found 500 equally parsimonious trees. To ascertain the level of phylogenetic support in the data 500 nonparametric bootstrap replicates were generated and their consensus calculated. The 50% majority-rule consensus of the 500 equally parsimonious trees is given in Figure S3b. Groups are collapsed when they are found in fewer than 50% of the equally parsimonious trees. The numbers above the branches represent the frequency of that group among the equally parsimonious trees. The numbers below the branches (or to the right of the sequence IDs when internal branches were short) are the bootstrap support percentages. Bootstrap support values less than 70% are not shown.

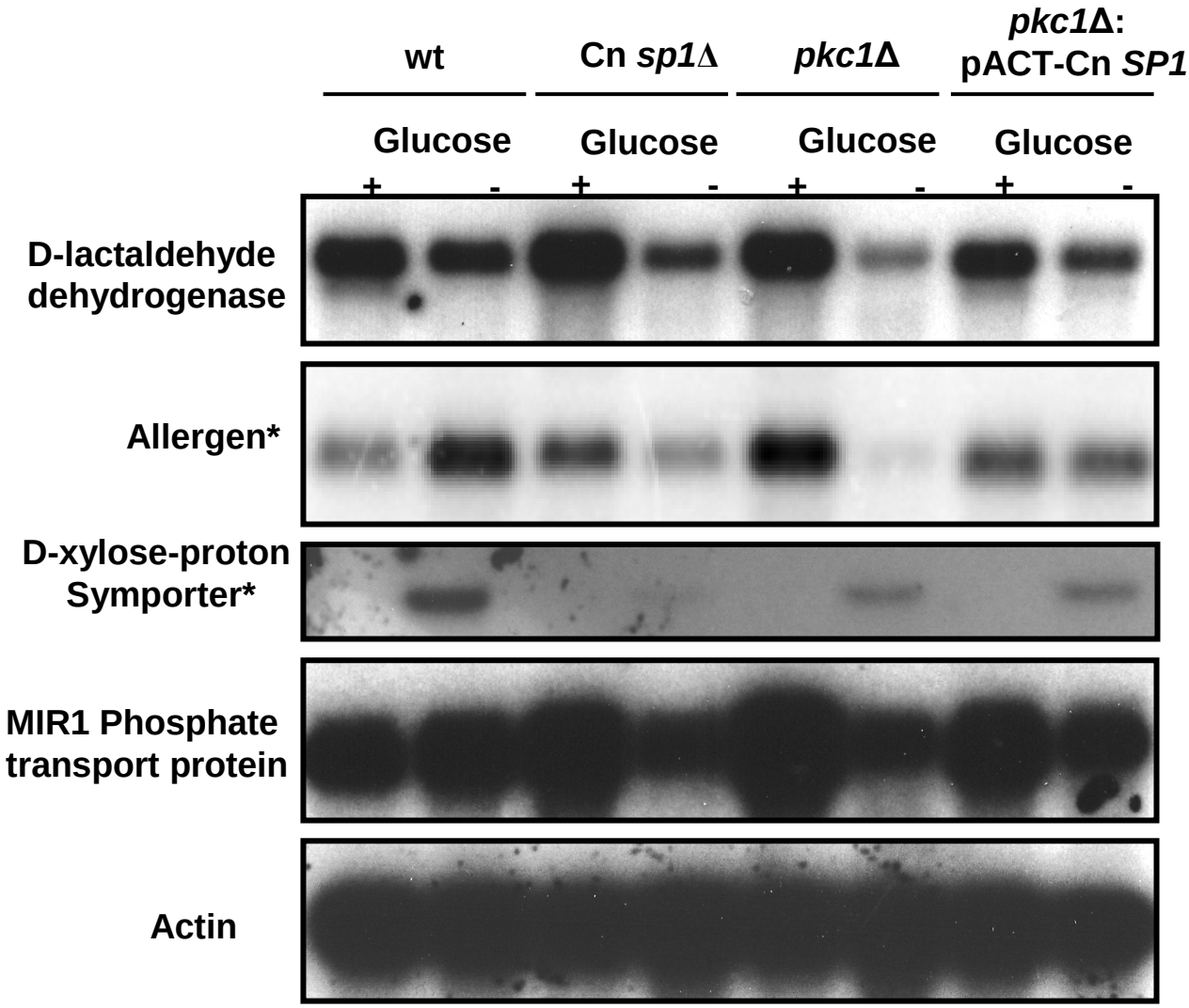

Figure S4a. Northern blot validation of genes in microarray experiments.

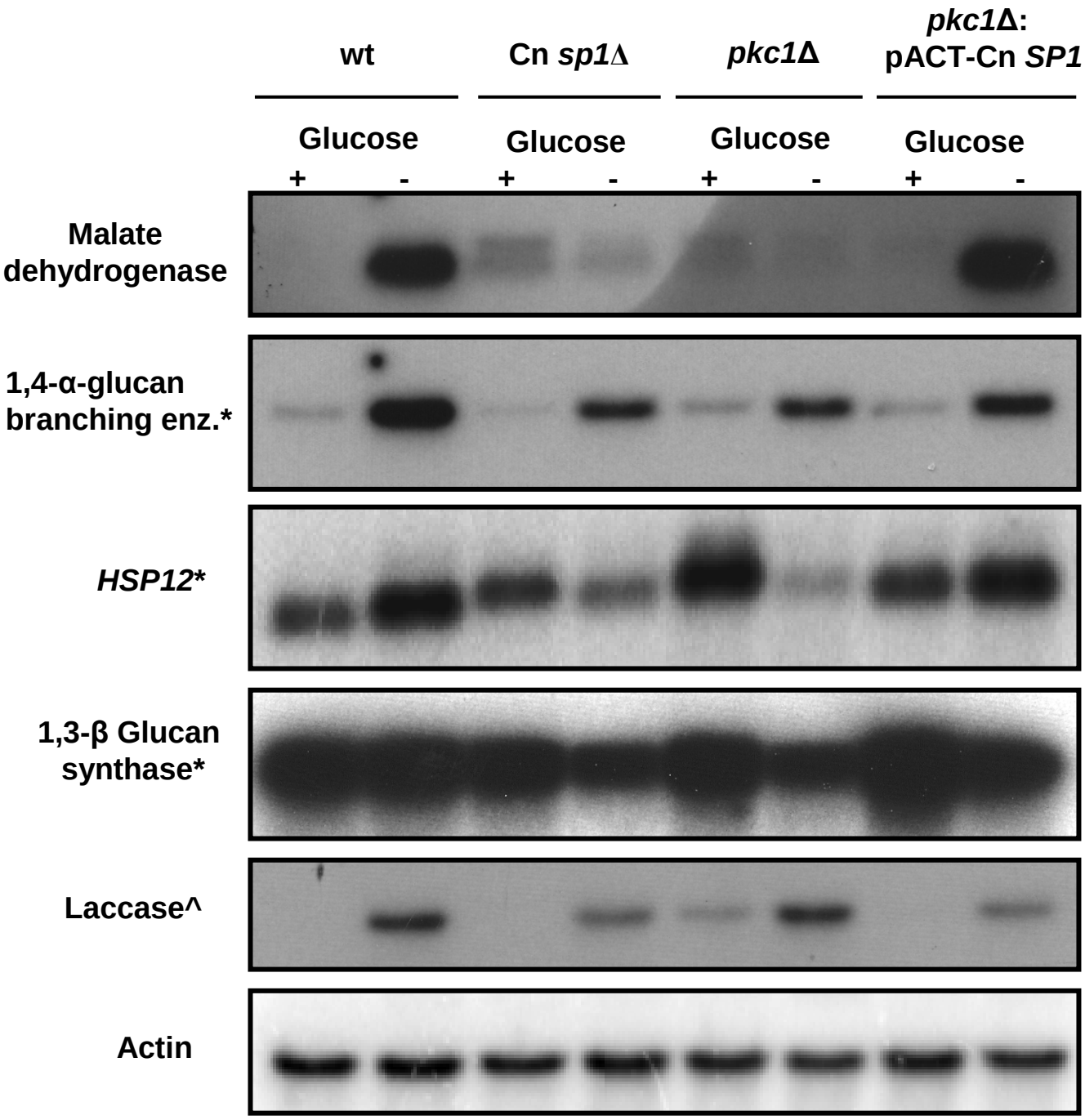

Figure S4a. Northern blot validation of genes in microarray experiments.

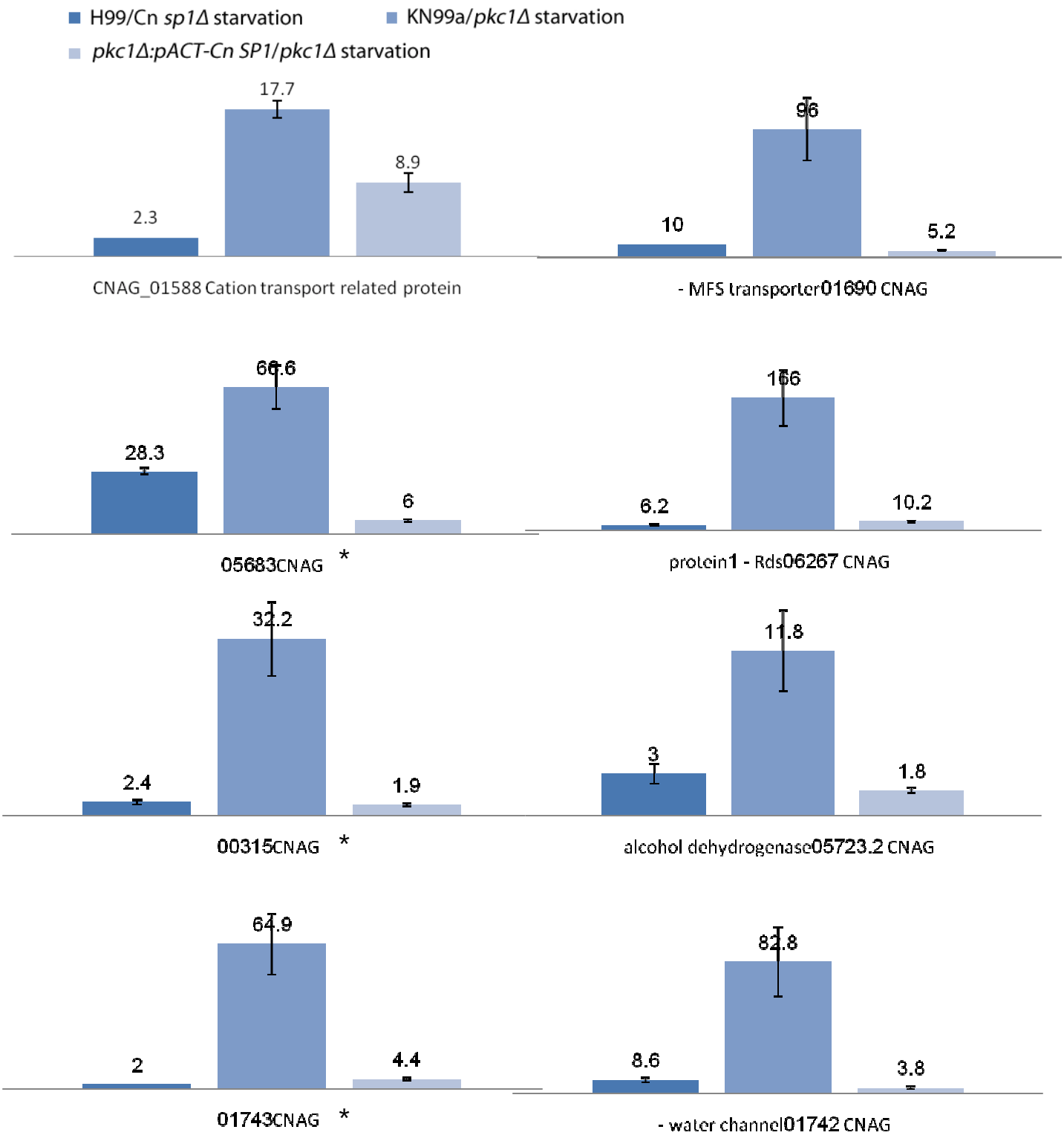

Figure S4b. qRT-PCR validation of genes in microarray experiments.
Results represent normalized expression (ΔΔCt+/-SD) in starvation of the following strains/conditions (with *ACT1* as control): wt (H99)/Cn *sp1Δ*, wt (KN99)/*pkc1*Δ, and *pkc1*Δ:pACT-Cn *SP1*/ *pkc1*Δ.

*Denotes genes that were identified in both microarray studies. NAD-dependent malic enzyme had an FDR of >0.05 but was also chosen based on interest.

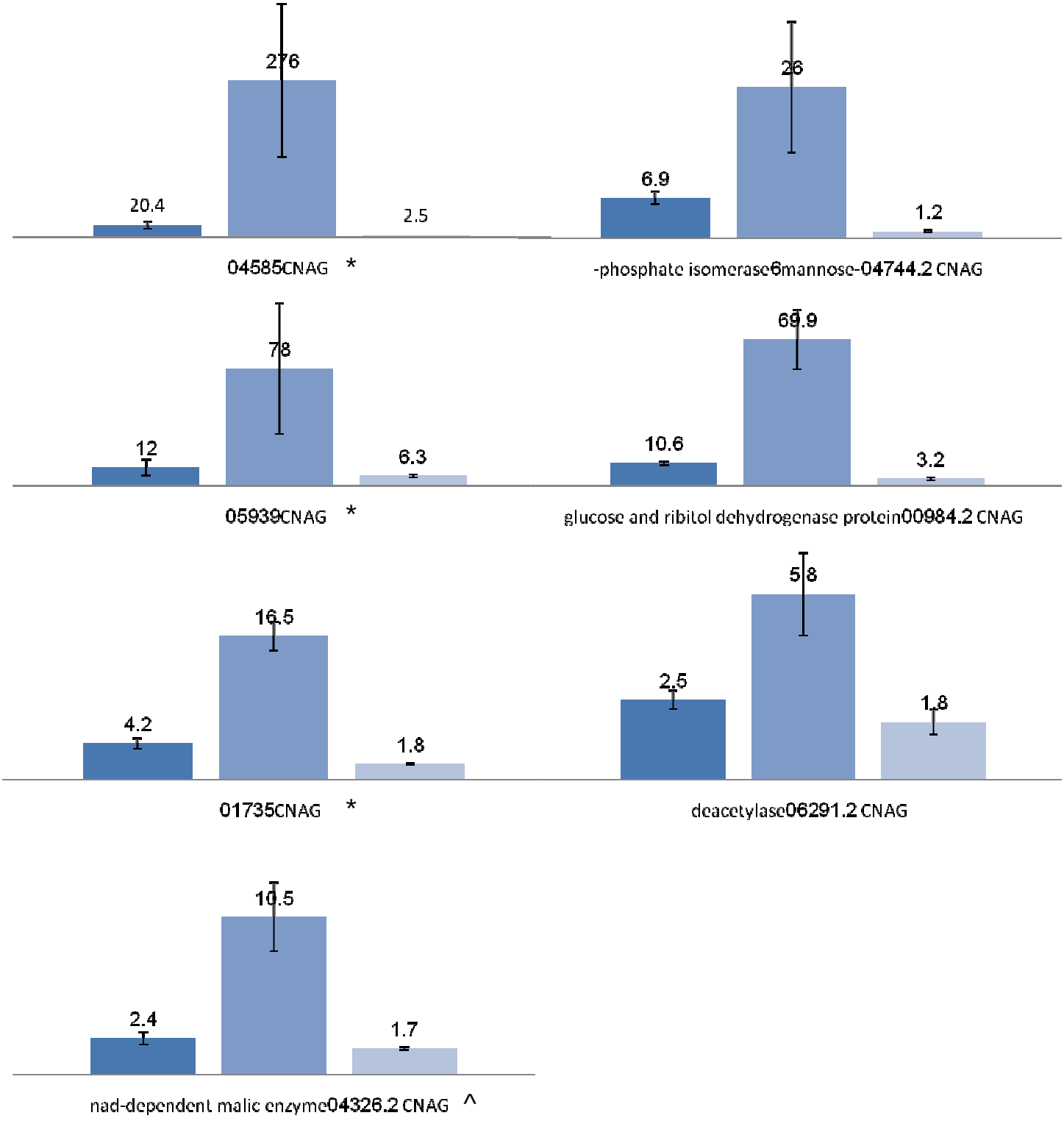

Figure S4b (con't)

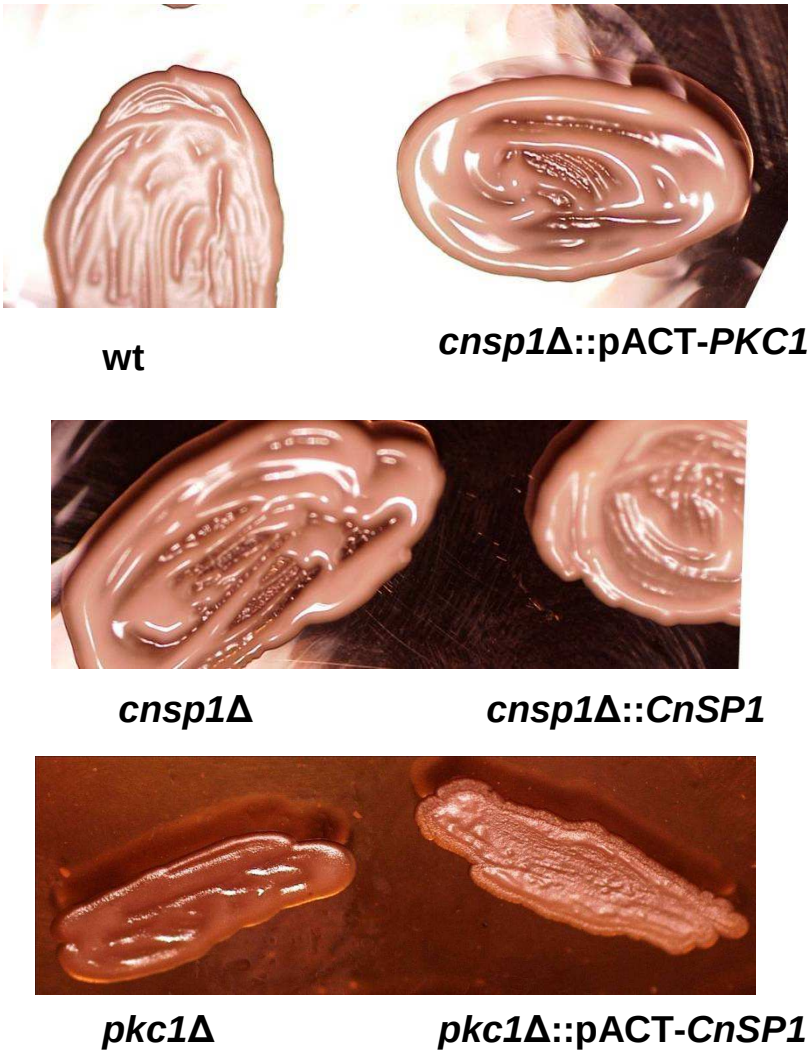

Figure S5. Cn *sp1Δ (cnag00156Δ)* and *pkc1Δ* demonstrates mucoid morphology . WT (H99), *cnag00156Δ* (designated Cn *sp1Δ*), *pkc1Δ,* Cn *sp1*Δ:Cn *SP1*, *pkc1*Δ:pACT-Cn *SP1*, and Cn *sp1*Δ:pACT-*PKC1* strains were grown on YPD + Sorbitol media (non-capsule inducing condition) and photographed.

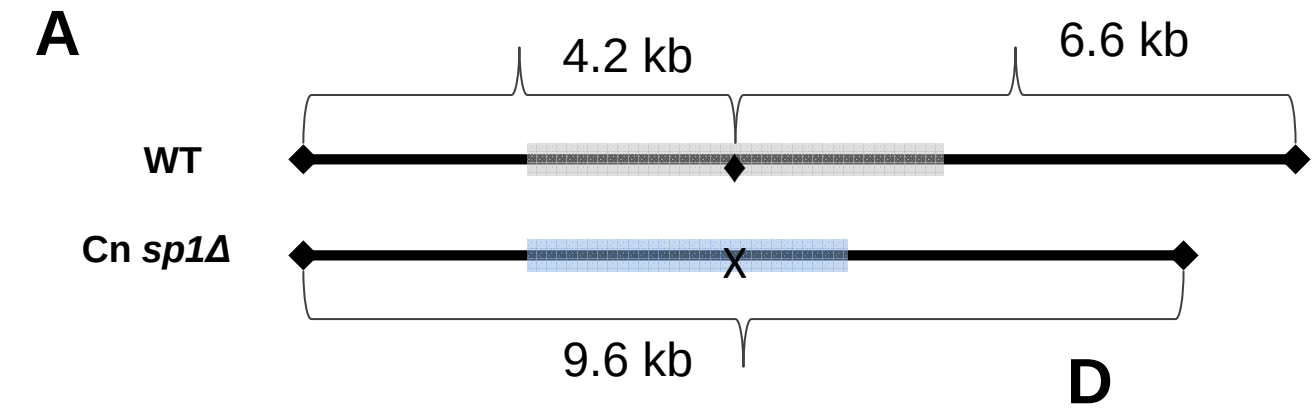

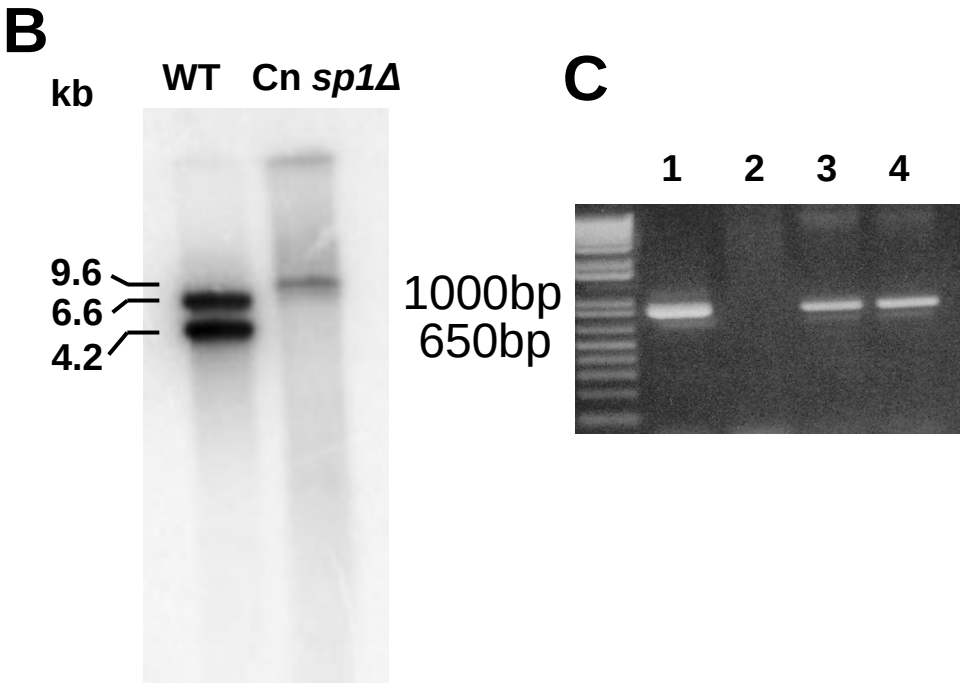

Figure S6. Generation of Cn *SP1* knockout and its complementation.
(A) Map WT vs. Cn *sp1Δ* genetic regions. *Mun*I sites are marked with a diamond sign. Cn *SP1* coding region and knockout construct are marked with grey and blue, respectively. **(B)** Southern blot of wt and Cn *sp1Δ* strains digested with *Mun* I. Hybridization fragment included the 1st and last 500bp of the Cn *SP1* coding region (primers detailed in 'experimental procedures'), to allow detection of both WT and mutant. In the WT fragment, a *Mun*I site, located 2076bp into the ORF lead to detection of 2 separate bands. In Cn *sp1Δ*, the WT ORF was replaced with a ~2.4 construct lacking a *Mun*I site (marked 'x'), leading to only one band.
(C) Lack of Cn *SP1* transcript in Cn *sp1Δ*. DNAse-treated RNA was extracted from H99 (lanes 1,3) and Cn *sp1Δ* (lanes 2,4) cells, followed by reverse transcription and PCR of Cn *SP1* (lanes 1,2) and *SSA1* (lanes 3,4) as control. Cn *SP1* cDNA is amplified in H99 but not in Cn *sp1Δ*.
(D) Southern blot (uncut) of Cn *sp1Δ* complementation demonstrates episomal location of Cn *SP1* expression construct in two strains (lane 1 and lane 2). Probe of Cn *SP1* was design to detect a fragment not present in the mutant, using primers Crz1probe 1608S (5'- CCACAATCCCATCCTTTACCAC) and Crz1probe 2465A (5'- AACCGACTTACCCGCAAACG). Lane 1-WT; 2-5-complemented strains; 6- Cn *sp1Δ*. Genomic DNA localized in reference to Ethidium bromide-stained gel.

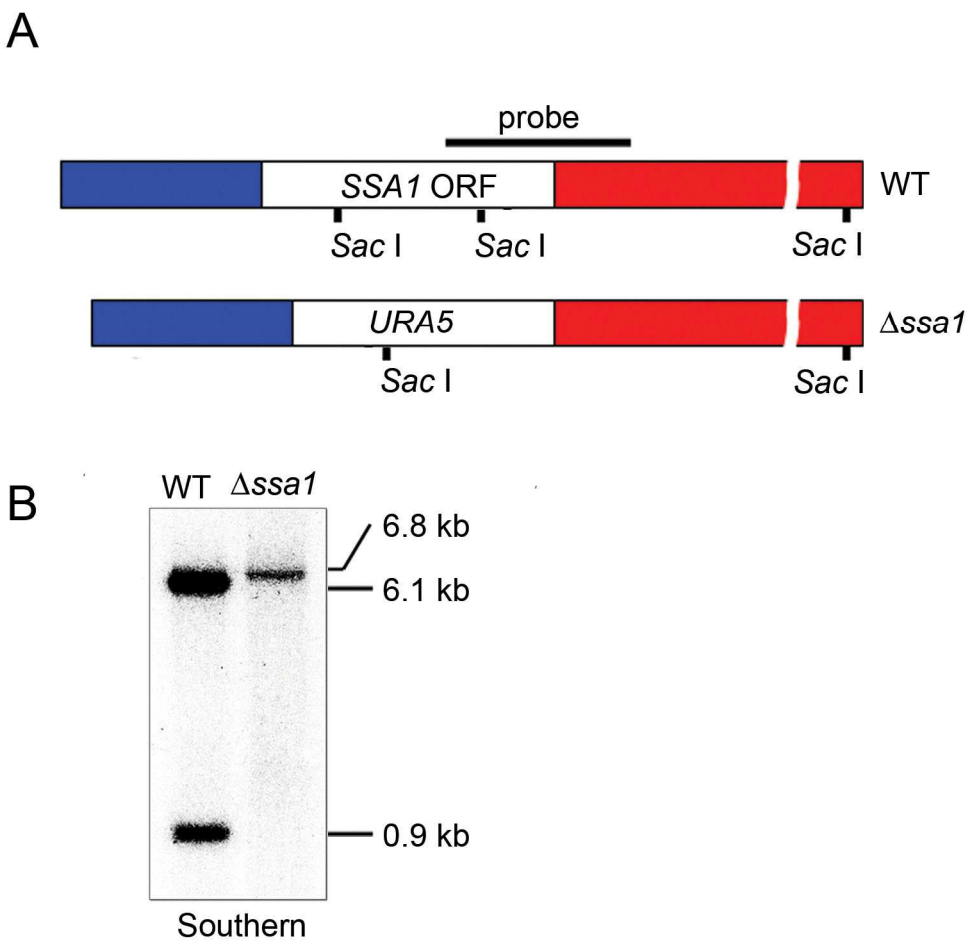

Figure S7. Generation of *SSA1* knockout strain.
(A) Schematic drawing of the *SSA1* locus in the WT and the *ssa1Δ* strains, outlining the location of the Southern blot probe shown in B and *Sac*I restriction sites.
(B) *Sac*I-cut Southern blot of the WT and the *ssa1Δ* strains, probed to the location outlined in A.

Supplemental Methods:

Generation of a SSA1 knockout strain-Standard methods were used for disruption of the *SSA1* gene, as described previously (Hu et al., 2008). Briefly, to make the deletion construct, 2 PCR-amplified fragments of the Cn SSA1 (using primers SSA1-up-Xba I-s, 5′-TTATCTAGACTTGAACGTAAA GCTAAGAG, and SSA1-up-Bgl II-a, 5′-TAAAGATCTTTATCTATTAAAGCTTTG AG; SSA1-down-EcoR I-s, AGCGAATTCCAAGGCGTAGTAATAAAAGG, and SSA1-down-Xho I-a, 5′-TATCTCGAGTGTTGACGAGAGAGATGGAG), the first digested with *Xba* I and *Bgl* II and the second digested with *Eco*R I and *Xho* I, was mixed with a 1.3-kb PCR fragment of the *C. neoformans URA5* gene described previously (Hu et al., 2008), digested with *Bgl* II and *Eco*R I and ligated to BlueScript SK digested with *Xba* I and *Xho* I. The final disruption allele with a 1.3-kb *URA5* marker flanked on either side by a 500-bp DNA sequence homologous to genomic regions of the *SSA1* gene was PCR-amplified and introduced into H99FOA cells via a biolistic approach (Cox et al., 1996) to effect a 2.2-kb deletion within the *SSA1* coding region. Transformants were screened for potential *SSA1* deletion mutant by a PCR, and the specific disruption of the *SSA1* gene in candidate mutant was verified by Southern blot analysis (Figure S6b).

Construction and use of an H99 three probe microarray: Construction and use of an H99 two-probe microarray: Cryptococcus neoformans var grubii H99 transcript sequences were downloaded from the BROAD Institute website. Hybridization probe sequences(60-mer) were selected using e-Array software (Agilent): two for each of the 6,969 transcripts, one of them strongly 3-prime biased (“best probe methodology”) the other less so (“best distribution methodology”). The 13,938 unique probes were arrayed in 3 replicate, randomized, locations on the Agilent Sure-Print microarray slide, 4x44K format. Additional control probes were included as well. (This array design has been deposited in GEO, accession GPL11486, as well as the mAdb NIH microarray database, internal name “Cnda”). Cy dye labeled hybridization target material was prepared from 10 ug total RNA and hybridized at 65o C for 17 hrs using TECAN 4800 HS Pro robotic hybridization station operating “Agilent GE 17 hrs” program. Slides were dried and maintained under nitrogen until scanning at 5 um resolution using Agilent G2505C. Agilent Feature Extraction software (protocol GE2_107_Sep09) was used for image analysis. Co-hybridizations were performed according to a common reference design with pooled sample in Cy5 channel on each array. Replicate RNA samples from two independent experiments for each condition. SAS and JMP-Genomics software (SAS, Cary NC) was used for statistical analysis. Starting with Agilent Feature Extraction "processed signal" (normalized) data, one channel per sample, we calculated the median signal for each locus ID (3 replicates of 2 unique probes) and transformed to log2. A mixed effects ANOVA model (fixed effect of strain-condition, random effect of array_ID) was computed for each gene over 24 different strain/growth conditions, and expression difference estimates calculated for the comparisons of interest. False Discovery Rate (FDR) estimates were based on the raw p-values for the 6,969 gene-wise tests over 5 treatment group comparisons. The genes called significantly different with FDR of 0.05 had a raw p-value < 0.03.